# Interior structure transfer via harmonic 1-forms

**Juncong Lin · Jiazhi Xia · Xing Gao · Minghong Liao ·
Ying He · Xianfeng Gu**

**Abstract** As a natural extension of surface parameterizaiton, volumetric parameterization is becoming more and more popular and exhibiting great advantages in several applications such as medical image analysis, hexahedral meshing etc. This paper presents an efficient volume parameterization algorithm based on harmonic 1-form. Our new algorithm computes three harmonic 1-forms, which can be treated as three vector fields, such that both the divergence and circulation of them are zero. By integrating the three harmonic 1-forms over the entire volumes, we can bijectively map the volume to a cuboid domain. We demonstrate the power of the technique by introducing a new application, to transfer the interior structure during the morphing of two given shapes.

J. Lin · X. Gao · M. Liao
Software School, Xiamen University, Xiamen, People's Republic of China

J. Lin
e-mail: jclin@xmu.edu.cn

X. Gao
e-mail: gaoxing@xmu.edu.cn

M. Liao
e-mail: liao@xmu.edu.cn

J. Xia (✉)
School of Information Science and Engineering, Central South University,
Changsha, Hunan, People's Republic of China
e-mail: xiajiazhi@gmail.com

Y. He
School of Computer Engineering, Nanyang Technological University, Singapore, Singapore
e-mail: yhe@ntu.edu.sg

X. Gu
Department of Computer Science, Stony Brook University, Stony Brook, NY 11790, USA
e-mail: gu@cs.sunysb.edu

# 1 Introduction

Parameterization technique has been an important role in computer graphics community for decades. The initial driving force of parameterization technique was texture mapping, to enhance the visual quality of polygonal models. Later on, other applications such as surface approximation and remeshing have stimulated further developments as the quickly developing of 3D scanning technology demanding for efficient compression methods of increasingly complex triangulations.

There have been a lot of surface parameterization techniques after decades development. However, the volumetric domain has not drawn too much attention until recently. In fact, most real-world shapes are volumetric. The needs for volumetric parameterization is ubiquitous in various research fields. In medical imaging, for example, the registration between two 3D image data sets can be reduced to building a map between their underlying parameter domains. In finite element simulations, hexahedral meshes are a highly desired representation for volumes, while such a mesh can be easily built out of the parameterization using certain canonical domains.

In this paper, we present a harmonic 1-form based volumetric parameterization algorithm. Our volumetric parameterization algorithm computes three harmonic 1-forms, which can be treated as three vector fields, such that both the divergence and circulation of them are zero. By integrating the three harmonic 1-forms over the entire volumes, we can bijectively map the volume to a cuboid domain. Compared to the existing volume parameterization techniques, e.g., [23, 31, 32], the proposed algorithm is efficient, because intrinsically, the algorithm is to solve sparse linear systems. Furthermore, the resulted parameterization is guaranteed to be bijective and singularity free.

We demonstrate the power of our algorithm by introducing a new application: to transfer the interior structure during the morphing of two given shapes. Morphing is a very popular technique in computer graphics, various algorithms have been proposed to realize and improve such a special effect. However, to our knowledge, all the existing methods focus on the generation of the intermediate shapes between two given surface models. No work has been done on the transfer of *internal* structure of intermediate shapes. In fact, it is highly desirable to transfer the internal structure during shape transformation. For example, it can be used to show how the skeleton changes when a person grows up from a child to an adult in medical applications, or how the specie evolves in biology applications.

Equipped with the 1-forms volumetric parameterization technique, we can realize a framework for transfer of the interior structure. Given the source shape $M_1$, let $\partial M_1$ denote the boundary surface and $I_1 \subset M_1$ the interior structure of interests. The target shape $S_2$ is given by the boundary surface $\partial M_2$. We first find a bijective map $\phi : \partial M_1 \to \partial M_2$ between boundary surfaces $\partial M_1$ and $\partial M_2$. Then we find the bijective map between two volumes $\psi : M_1 \to M_2$ using the boundary map constraint $\phi$, such that $\psi|_{\partial M_1} = \phi$. Next, the interior structure $I_1$ is transferred to $M_2$ using the volume
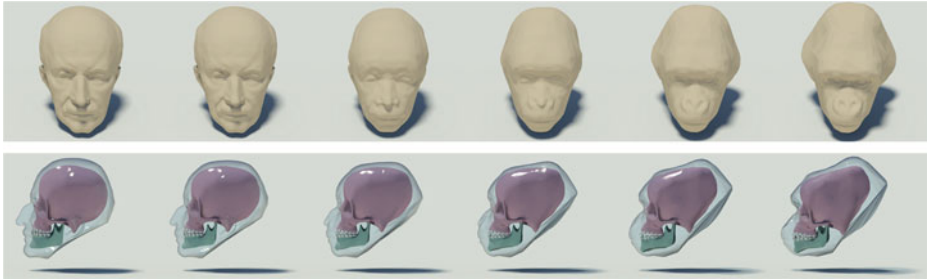
**Fig. 1** The volume parameterization induces the transfer of the interior structure between the human head and gorilla head

parameterization $\psi$. An as-rigid-as-possible deformation method is applied to avoid the artifacts near the boundary surface. We finally generate the interior structure of each intermediate shape by linear interpolation. Figures 1, 9, 10 are some results generated with our framework.

The main contributions of this paper includes:

– We propose a harmonic 1-form based method to parameterize topological ball to a cuboid domain. The proposed method is efficient and can guarantee the map to be a diffeomorphism.
– We develop a framework that can transfer the interior structure between two genus-0 handlebodies. By taking advantage of the diffeomorphism property of the volume parameterization and an as-rigid-as-possible deformation method, the transfer is smooth and free of artifacts.

The rest of this paper is organized as follows. We briefly review the related work in Section 2 and introduce the theoretical background of harmonic forms in Section 3. We present the harmonic 1-form based volume parameterization in Section 4. Section 5 shows the framework of interior structure transfer. The experimental results and discussions are presented in Section 6. Finally, we conclude our work and highlight the future work in Section 7.

## 2 Related work

### 2.1 Surface parameterization

Surface parameterization has been extensively studied in the past decades. The survey papers by Sheffer et al. [18] and Floater and Hormann [5] are good reference for general interests. Harmonic map is an important technique that maps a topological disk to a convex 2D domain [9, 10, 16]. To parameterize surfaces of arbitrary topology, Gu and Yau pioneered the global conformal parameterization that computes the holomorphic 1-form (a complex 1-form such that both the real and imaginary parts are harmonic) for each cohomology class [8]. Tong et al. extended

the space of harmonic 1-form that allows line singularities and singularities with fractional indices and presented an algorithm to construct quadrilateral meshes [24]. Tarini et al. pioneered the concept of Polycube maps to minimize both the angular distortion and area distortion [21]. Since then, various effects have been made for Polycube maps construction [13] and application [14, 27, 28].

## 2.2 Volume parameterization

Due to its great potential in several applications such as solid texture mapping, volumetric tetrahedralization for simulation and 3D image data process etc., volume parameterization attracts more and more attentions. Recently, it has also been adopted in data management of Wireless Sensor Networks(WSNs) to conquer the failure of in-network data management schemes when facing with communication voids in WSNs [17, 34].

Wang et al. generalized the surface harmonic map to volumes and derived the formula of the the discrete harmonic map on tetrahedral meshes [26]. Li et al. used the method of fundamental solution to solve the harmonic map between volumes in a meshless manner [31, 32]. In sharp contrast to the surface harmonic map, volumetric harmonic map can not guarantee the bijection even though the co-domain is convex. Thus, the above methods may not work well for the interior structure transfer due to the artifacts caused by the non-bijectivity.

Martin et al. presented a different way to parameterize volumes to cylindrical domain [23]. By choosing a 1-dimensional skeleton inside the volume, they solved a harmonic map using the skeleton and the boundary surface as the boundary constraints. Then, they traced the gradient field of the harmonic function and constructed a map between the volumes and the cylinder. Although this method can produce a bijection, the skeleton is the singularity of the constructed map. Furthermore, tracing the vector field inside the volume is computational expensive.

Xia et al. [29] presented a technique for parameterizing star-shaped volumes using the Green's functions. They show that the Green's function on the star shape has a unique critical point and prove that the Greens functions can induce a diffeomorphism between two star-shaped volumes. They developed algorithms to parameterize star shapes to simple domains such as balls and star-shaped polycubes, and demonstrated the technique in applications such as volumetric morphing and anisotropic solid texture transfer.

Later on, Xia et al. [30] presented a volumetric parameterization for 3-dimensional handlebodies that can be decomposed into the direct product of 2-dimensional surface and a 1-dimensional curve. They first partition the boundary surface into ceiling, floor and walls. Then harmonic field is computed in the volume with a Dirichlet boundary condition. By tracing the integral curve along the gradient of the harmonic function, the volume is parameterize to the parametric domain. The method is guaranteed to produce homeomorphism for various handlebodies with complicated topology, including topological balls as a degenerate case. Furthermore, the parameterization is regular everywhere. The advantage of the method is demonstrated in hexahedral mesh generation and volumetric check-board texture mapping.

Han et al. [11, 12] developed a method to construct layered hexahedral mesh for shell objects based on the volumetric parameterization of shell space. Given a

closed 2- manifold and the user-specified thickness, they constructed the shell space using the distance field and then parameterized the shell space to a polycube domain. The volume parameterization induced the hexahedral tessellation in the object shell space. As a result, the constructed mesh was an all- hexahedral mesh that most of the vertices are regular, i.e., the valence is 6 for interior vertices and 5 for boundary vertices. The mesh also had a layered structure that all layers had exactly the same tessellation.

Gregson et al. [6] presented a deformation-driven framework to build the volumetric mapping between the input model and a PolyCube. Given an isotropic tetrahedral mesh of an object, they firstly aligns the model's surface normals with one of the six global axes with a rotation-driven deformation while preserving shape as much as possible. Then an position-driven deformation is applied to extract a PolyCube structure from the sufficiently axis-aligned shape. The deformation gradients are propagated into the interior vertices during the two deformation step. From the PolyCube structure and mapping between the input model and the PolyCube, they can automatically generate good quality all-hex meshes of complex natural and man-made shapes.

Nieser et al. [15] first designed a frame field with manual input from the designer, then used the field to guide the interior and boundary layout of a volume parameterization. Finally, the parameterization and the hexahedral mesh are computed so as to align with the given frame field. Theoretical conditions on the singularities and the gradient frame-field are also derived.

Zeng et al. [35] presented volumetric colon wall unfolding, an efficient and effective volumetric colon unfolding method based on harmonic differentials. The method could be used for virtual colon analysis and visualization with valuable applications in virtual colonoscopy (VC) and computer-aided detection (CAD) systems.

Compared to the existing approaches, the proposed harmonic 1-form based volume parameterization is efficient as the volumetric harmonic map [26] since it only solves three sparse linear systems. On the other hand, it also guarantee the parameterization to be diffeomorphic as the vector field tracing approach [23].

## 2.3 Shape morphing

Depending on the shape representation, shape morphing methods can be roughly classified into two groups: boundary mesh methods and implicit surface method. The former usually relies on an explicit parametrization between meshes, e.g. [1, 33]. The shape is then transformed from one mesh to the other by moving points along the parameterized paths of correspondence. Thanks to the explicit mapping, attached properties such as color can also be transferred easily. The main limitation of these methods is that they can not handle the change of topology well. In contrast, implicit surface based methods (e.g., [3, 25]) can handle topology change elegantly and thus gains more popularity. However, there are no mappings between points of the different shapes in the transformation. Several methods have been proposed to resolve the mapping problem for implicit morphing [4, 22].

Although there have been a lot of research efforts on morphing, none of them discuss the transfer of internal structures. To our knowledge, our work is the first to address this problem.

## 3 Theoretic background

This section presents the mathematical background of the discrete harmonic 1-forms which will be used heavily in our volume parameterization algorithm. Suppose $M$ is a simplicial complex. We use $[v_0, v_1, \cdots, v_n]$ to represent a *n-simplex*. For example, vertex, edge, face and tetrahedron are simplecies.

### 3.1 Closed and exact forms

A *k-chain* $\gamma_k$ is a linear combination of all $k$-simplices in $M$, $\gamma_k = \sum_i c_i \sigma_i^k$. All $k$-chains form a linear space, called the *k dimensional chain space* $C_k$. The *k-dimensional boundary operator* $\partial_k : C_k \rightarrow C_{k-1}$ is a linear operator, defined as taking the boundary of a $k$-chain,

$$\partial_k \left( \sum_i c_i \sigma_i^k \right) = \sum_i c_i \partial_k(\sigma_i^k),$$

where $\sigma_i^k$ goes through all $k$-simplicies in $M$. On each simplex,

$$\partial_k [v_0, v_1, \cdots, v_k] = \sum_{i=0}^{i} (-1)^i [v_0, \cdots, \tilde{v}_i, \cdots, v_k],$$

where $[v_0, \cdots, \tilde{v}_i, \cdots, v_k]$ represents the $(k-1)$-simplex with vertices from $v_0$ to $v_k$ except $v_i$.

A *k-form* is a linear function defined on the chain space, $\omega_k : C_k \rightarrow R$,

$$\omega_k(\gamma_k) = \omega_k \left( \sum_i c_i \sigma_i^k \right) = \sum_i c_i \omega_k(\sigma_i^k).$$

Sometimes, the action of $\omega_k$ on $\gamma_k$ is also denoted as $< \omega_k, \gamma_k >$. All $k$-forms form a linear space, the so-called *k-dimensional co-chain space* $C^k$. The *k dimensional co-boundary operator* $d_k : C^k \rightarrow C^{k+1}$ is a linear operator, defined as the dual operator of the boundary operator $\partial_{k+1}$,

$$< d_k \omega_k, \gamma_{k+1} > = < \omega_k, \partial_{k+1} \gamma_{k+1} > . \tag{1}$$

The above equation is called the *Stokes formula*.

Suppose $\omega$ is a $k$-form, then $\omega$ is an *exact form*, if there exists a $(k-1)$-form $\tau$, such that $\omega = d_{k-1} \tau$; $\omega$ is a *closed form*, if $d_k \omega$ is 0. It can be verified easily that all exact forms are closed. Let $\omega_1$ and $\omega_2$ are closed $k$-forms, if they differ by an exact $k$-form, $\omega_1 - \omega_2 = d\tau$, then they are *cohomologous*. All the cohomologous classes of closed $k$-forms form the *k dimensional cohomology group* of $M$. Symbolicly,

$$H^k(M, R) = \frac{ker d_k}{img d_{k-1}},$$

where $ker d_k$ represent the kernel of $d_k$, which is the linear space of all closed $k$-forms; $img d_{k-1}$ represents the image of $d_{k-1}$, which is the linear space of all exact $k$-forms.

3.2 Harmonic forms

Suppose $M$ is embedded in $R^3$, $f : C_0 \to R$ is a 0-form on $M$, namely, a function defined on vertices. Then $f$ can be extended to a piecewise linear function on $M$. The *harmonic energy* of $f$ is defined as

$$E(f) = \int_M |\nabla f|^2 dv,$$

where $\nabla f$ is the gradient of $f$, $dv$ is the volume element on $M$. ($f$ is piecewise linear, therefore $\nabla f$ is well-defined on the interior points of all simplices, the singular sets of $\nabla f$ is of zero measure, the integration is well defined.) A *harmonic function* is a critical point of the harmonic energy.

Let $[v_i, v_j]$ be an edge in $M$, $\theta_{kl}^{ij}$ represent the dihedral angle on edge $[v_k, v_l]$ in the tetrahedron $[v_i, v_j, v_k, v_l]$. The *edge weight* on $[v_i, v_j]$ is defined as

$$w_{ij} = \sum_{kl} l_{ij} \cot \theta_{kl}^{ij}.$$

where $l_{ij}$ is the edge length of $[v_i, v_j]$. Let $f$ be a 0-form, then *discrete Laplacian* of $f$ is a 1-form, defined as

$$\Delta f(v_i) = \sum_j w_{ij}(f(v_j) - f(v_i)) = \sum_j w_{ij}\omega([v_i, v_j]).$$

where $\omega = df$. It can be easily verified that harmonic functions have zero Laplacians.

Suppose $\omega$ is a closed 1-form, $\omega$ is harmonic if locally it is the discrete derivative of a harmonic function. Namely,

$$\forall i, \sum_j w_{ij}\omega([v_i, v_j]) = 0.$$

According to Hodge theorem [7], there exists a unique harmonic 1-form in each homologous class in $H^1(M, R)$. Our work focuses on finding three different harmonic 1-forms on $M$, whose existences are guaranteed by Hodge theory.

## 4 Harmonic 1-form based volume parameterization

Given a genus-0 handlebody $M = (V, E, F, T)$ where $V$, $E$, $F$ and $T$ are the vertex, edge, face and tetrahedron sets respectively, the volume parameterization $\psi : M \to \mathbb{R}^3$ is to assign a triplet $(u, v, w)$ to each mesh vertex.

Inspired by the global conformal parameterization [8] in which an exact harmonic 1-form and its conjugate are computed for each homotopy class, we parameterize the genus-0 handlebody as follows: first, we partition the boundary surface $\partial M$ into six patches, namely, front, back, top, bottom, left and right sides. Then, we compute two harmonic functions $u$ and $v$ using the front-back and left-right sides as Dirichlet boundary conditions. Next, we compute an non-exact harmonic 1-form $dw$ using the top-bottom constraint. We solve an optimization problem that scales the three harmonic 1-forms to make the three vector fields are locally as orthogonal as possible.

Finally, the parameters $(u, v, w)$ are obtained by integrating the 1-forms over the entire volume. The algorithm is shown in the following six steps, see also Fig. 2.

1. Partition the boundary surface into six patches.
2. Compute the harmonic 1-form using the front-back constraint.
3. Compute the harmonic 1-form using the left-right constraint.
4. Compute the harmonic 1-form using the top-bottom constraint.
5. Optimize the three harmonic 1-forms to make them as orthogonal as possible.
6. Integrate the three harmonic 1-forms over the entire volume to map it to a cuboid.

The algorithmic details are shown in the following subsections.

### 4.1 Boundary surface partition

This step is to partition the boundary surface $\partial M$ into six patches, $\Omega_i$, $i = 1, \cdots, 6$, which refer to front, back, left, right, top and bottom sides respectively. Although the partition is quite arbitrary from the theory point of view, to reduce the distortion, we do expect the partition follow the structure of the cuboid which is used as the parametric domain. Therefore, we parameterize the boundary surface $\partial M$ into a polycube which has very simple structure that facilitates the surface partition. In our implementation, we adopt the divide-and-conquer approach developed by He et al. [13]. With the polycube map, we allow the users to set the boundary patches by simple mouse clicks on the desired polycube faces.

### 4.2 Computing the harmonic 1-forms $\omega_0$ and $\omega_1$

To compute the harmonic 1-forms inside the volume using finite element method, we need to tetrahedralize the given shape $M$ using tetgen [19]. Then we apply the variational remeshing algorithm [2] to improve the mesh quality.
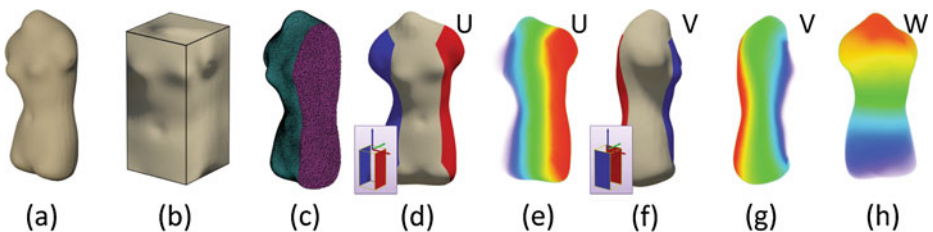


**Fig. 2** Pipeline of the harmonic-1 form based volume parameterization. **a** Input model $M$. **b** The polycube map of the boundary surface $\partial M$. **c** Construct the tetrahedral mesh of $M$ which is used to solve the harmonic functions. **d** The *left* and *right* sides. **e** Volume rendering of the $u$ parameter. **f** The front and back sides. **g** Volume rendering of the $v$ parameter. **h** Volume rendering of the $w$ parameter

With the tetrahedral mesh, we first compute the harmonic function $f_0 : M \to \mathbb{R}$ by solving the Dirichlet problem on the front and back sides, i.e., $\Omega_1$ and $\Omega_2$,

$$\begin{cases} f_0|_{\Omega_1} = 1 \\ f_0|_{\Omega_2} = 0 \\ \Delta f_0(v_i) = 0, \ v_i \notin \partial M \end{cases}$$

where $\Delta f_0(v_i) = \sum_j w_{ij}(f_0(v_j) - f_0(v_i))$. The gradient $\omega_0 = df_0$ is an exact harmonic 1-form.

Similarly, another exact harmonic 1-form $\omega_1$ can be computed by solving the following Dirichlet problem on the left and right sides,

$$\begin{cases} f_1|_{\Omega_3} = 1 \\ f_1|_{\Omega_4} = 0 \\ \Delta f_1(v_i) = 0, \ v_i \notin \partial M \end{cases}$$

Again, the gradient $\omega_1 = df_1$ is an exact harmonic 1-form.

### 4.3 Computing the harmonic 1-form $\omega_2$

Let $h$ be a 0-form (i.e., a scalar function) on $M$, such that $h|_{\Omega_5} = 1$ and $h|_{\Omega_6} = 0$, $h$ is arbitrary on other vertices. Then we define a closed 1-form $\omega$ on $M$, such that

$$\omega([v_i, v_j]) := dh([v_i, v_j]).$$

The harmonic 1-form $\omega$ is closed. Let $\omega_2$ be the unique harmonic 1-form on $M$ homologous to $\omega$. Then $\omega_2$ and $\omega$ differ by an exact 1-form $df_2$, where $f_2$ is a 0-form. By the harmonicity condition,

$$\sum_j w_{ij}(f_2(v_j) - f_2(v_i) + \omega([v_i, v_j])) = 0, \ \forall v_i \notin \partial M$$

the scalar function $f_2$ can be uniquely determined by solving the linear system. Therefore, harmonic 1-form $\omega_2 = df_2 + \omega$ can be constructed.

### 4.4 Optimizing 1-forms

After computing the harmonic 1-forms $\omega_0, \omega_1, \omega_2$, we convert them to three piecewise constant vector fields $\mathbf{e}_0, \mathbf{e}_1, \mathbf{e}_2$. Let $\omega$ be a closed 1-form, on each tetrahedron $[v_i, v_j, v_k, v_l]$, we find a vector $\mathbf{e}$, such that

$$\omega([v_i, v_j]) = < v_j - v_i, \mathbf{e} >$$

We find three constants $c_0, c_1, c_2$, such that the vector fields $c_0\mathbf{e}_0, c_1\mathbf{e}_1, c_2\mathbf{e}_2$ locally form a frame in $R^3$; the frame is as close to an orthogonal frame as possible. Therefore, we minimize the following energy:

$$E(c_0, c_1, c_2) = \sum_{i,j,k} \int_M |c_i c_j \mathbf{e}_i \times \mathbf{e}_j - c_k \mathbf{e}_k|^2 dv.$$

where $\{i, j, k\}$ traverse all the cyclic permutations of $\{0, 1, 2\}$.

For convenience, we still use $\omega_0, \omega_1, \omega_2$ to denote the scaled harmonic 1-forms.

### 4.5 Integration

The following integration algorithm flattens the volume $M$ to a cuboid. We denote the mapping as $\psi : M \to \mathbb{R}^3$.

1. Choose a base vertex $v_0$ in $\Omega_1$, set $\psi(v_0) = (0, 0, 0)$. Put $v_0$ in a queue.
2. While the queue is non-empty:

   (a) Pop the head of the queue, denoted by $v$.
   (b) Find all the neighboring vertices $w$.
   (c) If $w$ has not been accessed, compute
      $\psi(w) = \psi(v) + (\omega_0([v, w]), \omega_1([v, w]), \omega_2([v, w]))$.
   (d) Put $w$ in the queue.

Note that the above integration algorithm is simply the breadth-first searching algorithm, thus, can be executed very efficiently.

### 4.6 Diffeomorphic property

The proposed harmonic 1-form based volume parameterization can guarantee that the mapping is a diffeomorphism in the interior. We sketch the proof in the following.

Given the three harmonic 1-forms, $\omega_i$, $i = 1, 2, 3$, suppose $df_i = \omega_i$, where $f_i$s are harmonic functions with Dirichlet boundary conditions. According to maximal value principle, the harmonic functions $f_i$ reach extreme points on the volume boundary. Thus, there is no extremal point in the interior. Therefore, for any harmonic function $f_i$, the gradient of $f_i$, $df_i$ is non-zero in the interior.

Harmonic 1-forms are closed, therefore, they are integrable. The Jacobian matrix of the mapping $(x, y, z) \to (f_0, f_1, f_2)$ is given by $(df_0, df_1, df_2)^T$. Assume at some interior point p, the Jacobian matrix is degenerated, then there is a constant $\alpha_k$, such that

$$\alpha_0 du + \alpha_1 dv + \alpha_2 dw = (0, 0, 0)^T,$$

where $\alpha_k$'s are not all zeros.

Define $f = \alpha_0 f_0 + \alpha_1 f_1 + \alpha_2 f_2$, then $f$ is a harmonic function, and $f$ is not constant, because it has non-constant boundary values. But $\nabla f(p) = 0$, it has an extremal interior point p, contradiction.

Therefore, the Jacobian matrix is of full-rank for all interior points. According to inverse function theorem, the mapping is invertible. Because harmonic forms are infinitely smooth, therefore, the mapping is a diffeomorphism.

## 5 Interior structure transfer

We have detailed the 1-forms based volumetric parameterization technique in previous sections. In this section, we demonstrate the advantage of the new algorithm by applying the technique to the transfer of interior structure during shape transformation.

Figure 3 illustrates the flowchart of the interior structure transfer framework. We firstly map the source surface $\partial M_1$ and target surface $\partial M_2$ onto a common polycube domain which induces the consistent boundary partition of $\partial M_1$ and $\partial M_2$. Then,

**Fig. 3** Flowchart of interior structure transfer: *first row*, we parameterize the two given models onto polycube; *second row*, we can then generate a morphing sequence based on the polycube parameterization; *third row*, we do volumetric parameterization for the source shape $M_1$ and the target shape $M_2$; *fourth row*, the interior structure $I_1$ is embedded into $M_1$ and transferred to $M_2$ to generate $I_2$. The interior structure of each intermediate shape is then generated by linear interpolation of $I_1$ and $I_2$
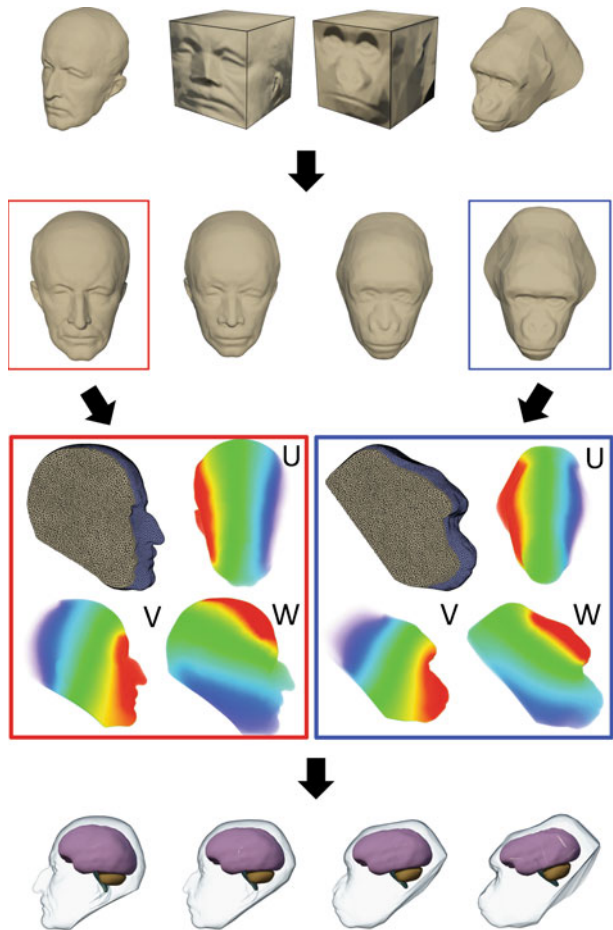


we parameterize $M_1$ and $M_2$ using the proposed volume parameterization method. Next, we embed $I_1$ into $M_1$ and the volume parameterization transfers $I_1$ to $M_2$. We finally generate the interior structures of intermediate shapes by linear interpolation between $I_1$ and $I_2$(the one transferred to $M_2$).

To transfer the interior geometric structure $I_1$ of shape $M_1$ to shape $M_2$, we firstly embed $I_1$ into $M_1$ by calculating the parameterization coordinate of each vertex $\mathbf{v}_i$ on the interior structure according to the mapping $f_1 : (x, y, z) \rightarrow (u, v, w)$:

$$\mathbf{u}_i^1 = f_1(\mathbf{x}_i^1)$$

The vertex position of each point in the transferred structure $I_2$ could then be computed by the inverse mapping $f_2^{-1} : (u, v, w) \rightarrow (x, y, z)$:

$$\mathbf{x}_i^2 = f_2^{-1}(\mathbf{u}_i^1) \tag{2}$$

Due to the distortion in parameterization, direct update of the vertex position in $I_2$ with such a simple method may lead to artifacts as shown in the first row of Fig. 4. We adopt a least-square strategy to update $I_2$ so as to eliminate the artifacts.

**Fig. 4** Elimination of artifacts: the *first row* shows the artifacts generated in direct update; the *second row* shows the improved result with as-rigid-as-possible update
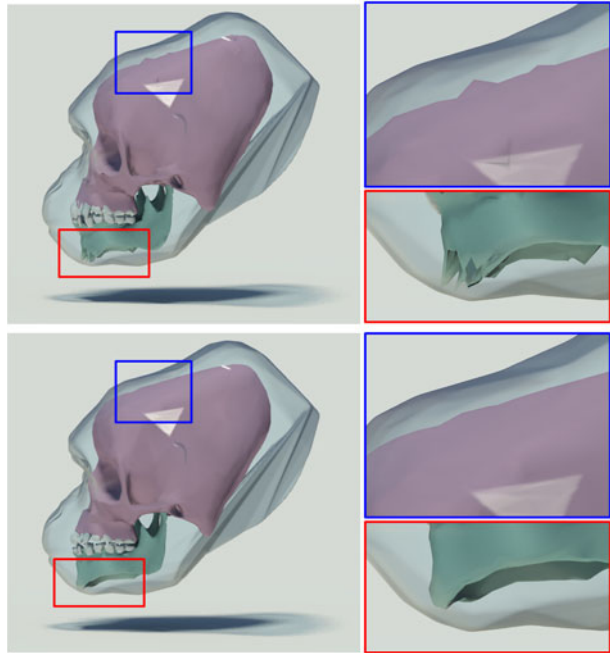


The basic idea is to initialize $I_2$ with $I_1$ and then deform $I_2$ in an as-rigid-as-possible manner [20] with the vertex coordinate computed by (2) as position constraints. The surface of $I_2$ is thought to be covered with small overllapping cells, and we try to find an ideal deformation that can keep the transformation for the surface in each cell as-rigid-as possible.

We define a cell $C_i$ as the one ring neighbour triangles of each vertices $\mathbf{v}_i$ in $I_1$. For cell $C_i$ and its deformed version $C_i'$, we could find an approximate rigid transformation $\mathbf{R}_i$ between the two cells by solving the following minimization problem:

$$E(C_i, C_i') = \sum_{j \in N(i)} w_{ij} \parallel (\mathbf{x}_i' - \mathbf{x}_j') - \mathbf{R}_i(\mathbf{x}_i^1 - \mathbf{x}_j^1) \parallel^2,$$

The cotangent weight formula is used for the weighting $w_{ij} = \frac{1}{2}(cot\alpha_{ij} + cot\beta_{ij})$. Denote $\mathbf{M}_i = \sum_{j \in N(i)} w_{ij}\mathbf{e}_{ij}\mathbf{e}_{ij}'^T$, the optimal rotation $\mathbf{R}_i$ could be derived from the singular value decomposition of $\mathbf{M}_i = \mathbf{U}_i \sum_i \mathbf{V}_i^T$ :

$$\mathbf{R}_i = \mathbf{V}_i\mathbf{U}_i^T.$$

The detail derivation could be found in [20].

We seek to minimize the following objective function during the deformation process:

$$E(S') = \sum_{i=1}^{n} w_i E(C_i, C_i') + \sum_{i=1}^{n} \parallel \mathbf{x}_i' - \mathbf{x}_i^2 \parallel^2 \tag{3}$$

The objective function consists of a rigid energy $E_r = \sum_{i=1}^{n} w_i E(C_i, C_i')$ and a positional energy $E_p = \sum_{i=1}^{n} \| \mathbf{x}_i' - \mathbf{x}_i^2 \|^2$. The partial derivatives of $E_r$ w.r.t $\mathbf{v}_i'$ could be written as:

$$\frac{\partial E_r}{\partial \mathbf{x}_i'} = \sum_{j \in N(i)} 4w_{ij} \left( (\mathbf{x}_i' - \mathbf{x}_j') - \frac{1}{2}(\mathbf{R}_i + \mathbf{R}_j)(\mathbf{x}_i^1 - \mathbf{x}_j^1) \right)$$

We then arrive the following overdetermined linear system by setting $\frac{\partial E_r}{\partial \mathbf{x}_i'} = 0$ and $\frac{\partial E_p}{\partial \mathbf{x}_i'} = 0$:

$$\begin{bmatrix} \mathbf{L} \\ \mathbf{W}_p \end{bmatrix} \mathbf{x} = \begin{bmatrix} \mathbf{r} \\ \mathbf{b} \end{bmatrix} \tag{4}$$

$L$ is the laplacian matrix of $I_2$, $W_p$ is a diagonal matrix filled by the positional weighting $w_p$. Both of them are $n \times n$ matrices, $n$ is the number of vertices in $I_2$. $r_i = \sum_{j \in N(i)} \frac{w_{ij}}{2}(\mathbf{R}_i + \mathbf{R}_j)(\mathbf{x}_i^0 - \mathbf{x}_j^0)$ and $b_i = w_p \mathbf{x}_i^2$.

To minimize (3), we firstly estimate the local rotation $\mathbf{R}_i$ with the vertex position calculated by (2) as the initial guess $\mathbf{x}_0'$. New position $\mathbf{x}'_1$ could be obtained by solving the linear system (4). We can iterative apply the process to further minimize the objective function. We conduct 5 iterations in our current implementation Because the rigid transformations $R_i$ only influence the right-hand side of the linear system, the system matrix only depends on the initial mesh. Thus we can firstly factorize the system matrix, and then perform back substitution only to solve the system.

## 6 Experimental results and discussions

We have implemented the techniques mentioned above with C++.

Figures 5, 6, 7 and 8 show extra volumetric parameterization results. Figures 1, 9 and 10 show more examples of interior structure transfer. Table 1 shows the statistics of volume parameterization, the program is run on a Pentium Xeon 2.67GHz CPU with 8.0G RAM. Compared with previous curve-tracing based method [12, 23, 29, 30], our method gains great advantage on efficiency. It only cost about half a minute in total to parameterize a tetrahedral mesh with the size around 90,000 vertices.
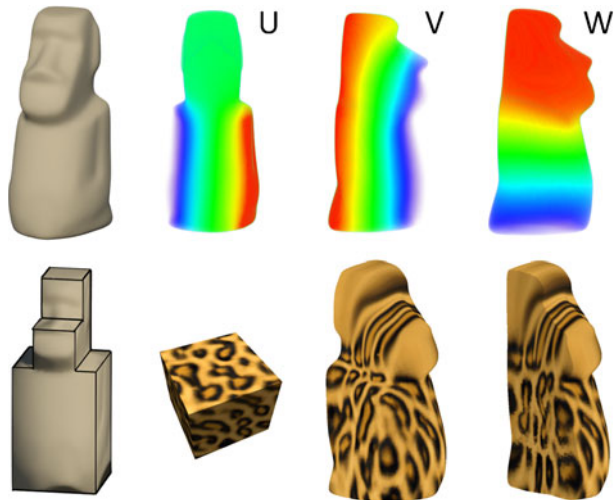


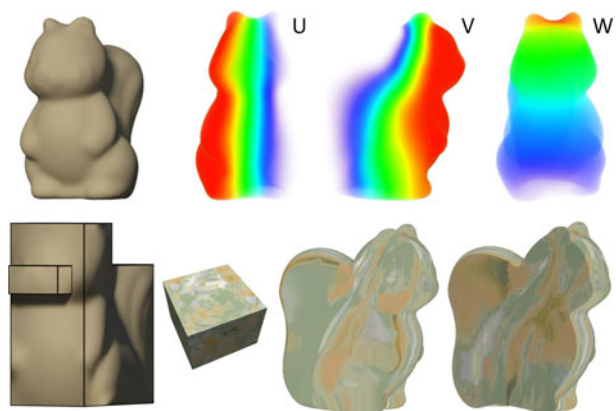**Fig. 5** Volume parameterization of pierrot model
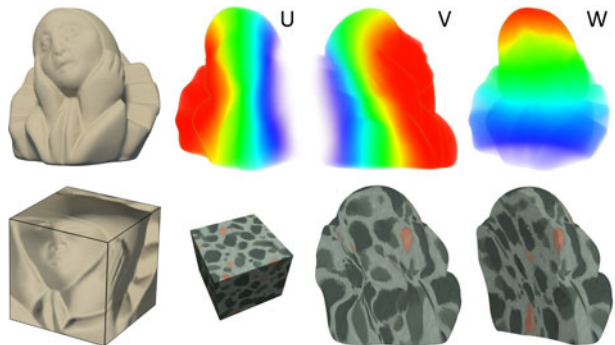
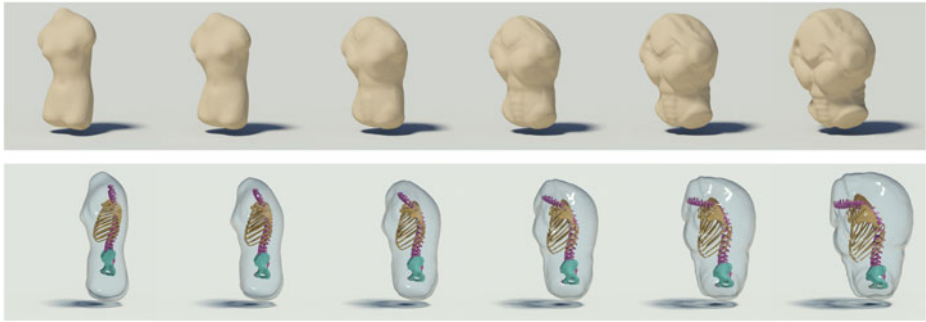**Fig. 6** Volume parameterization of maneki model
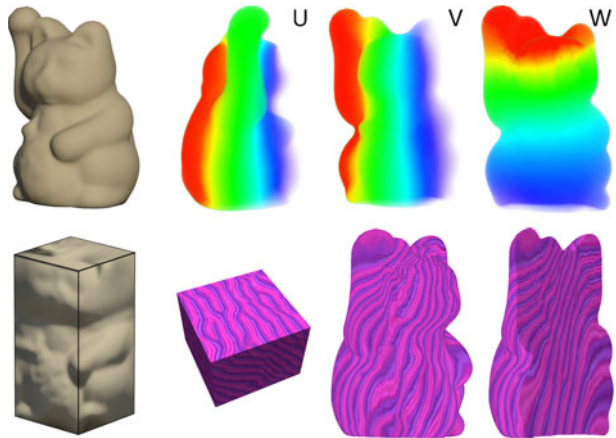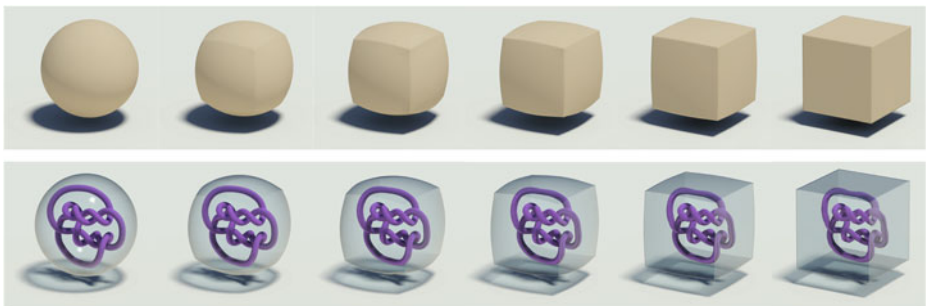


**Fig. 7** Volume parameterization of moai model



**Fig. 8** Volume parameterization of squirrel model

**Fig. 9** Transfer of torso skeleton from venus body to armadillo body



**Fig. 10** Transfer of knot structure from a sphere to a cube

**Table 1** Statistics of harmonic 1-form based volume parameterization

| Figure | | Size | Time (sec) | | |
|---|---|---|---|---|---|
| | | | u | v | w |
| Figure 1 | $\partial M_1$ | 90,031 | 3.9 | 3.7 | 15.3 |
| | $\partial M_2$ | 90,022 | 3.7 | 3.8 | 21.9 |
| Figure 5 | | 90,001 | 3.9 | 4.3 | 25.3 |
| Figure 6 | | 90,050 | 4.2 | 3.9 | 22.6 |
| Figure 7 | | 90,013 | 3.5 | 3.3 | 16.0 |
| Figure 8 | | 90,039 | 3.2 | 3.7 | 21.1 |
| Figure 9 | $\partial M_1$ | 90,000 | 3.3 | 2.9 | 18.6 |
| | $\partial M_2$ | 90,000 | 3.2 | 3.6 | 16.0 |
| Figure 10 | $\partial M_1$ | 90,004 | 3.9 | 4.1 | 18.8 |
| | $\partial M_2$ | 90,010 | 3.8 | 4.0 | 24.6 |

**Table 2** Statistics of interior structure transfer

| Figure | Size | Time (sec) |
|---|---|---|
| Figure 1 | 11,507 | 2.88 |
| Figure 3 | 3,477 | 0.87 |
| Figure 9 | 12,479 | 2.24 |
| Figure 10 | 5,808 | 1.89 |

Table 2 lists the statistics for the as-rigid-as-possible update of interior structure. The optimization only cost several seconds.

## 6.1 Limitations

There are still several limitations in our algorithm. One need to be listed separately is that our volumetric parameterization technique is only applicable for cuboid object. Obvious distortion may present for object far from a cuboid such as the example model shown in Figs. 7 and 8 (notice the large distortion of solid texture on the head part of the moai model).

## 7 Conclusions

A novel framework for the transfer of interior structure during shape transformation is presented in this paper. We firstly parameterize the source surface and the target surface onto a common polycube domain and generate a morphing sequence based on the correspondence of polycube map. We then generate tetrahedral mesh for both surfaces and conduct a harmonic 1-form based volume parameterization to construct a bijective mapping between the two volume space. After that, the interior structure is transferred from the source to the target based on the volume mapping. Finally, we generate the interior structures of intermediate shapes by linear interpolation between the source interior structure and the target interior structure.

## References

1. Alexa M, Cohen-Or D, Levin D (2000) As-rigid-as-possible shape interpolation. In: Proc ACM SIGGRAPH 2000, pp 157–164
2. Alliez P, Cohen-Steiner D, Yvinec M, Desbrun M (2005) Variational tetrahedral meshing. ACM Trans Graph 24(3):617–625
3. Cohen-Or D, Solomovic A, Levin D (1998) Three-dimensional distance field metamorphosis. ACM Trans Graph 17(2):116–141
4. Dinh HQ, Yezzi A, Turk G (2005) Texture transfer during shape transformation. ACM Trans Graph 24(2):289–310
5. Floater MS, Hormann K (2005) Advances in multiresolution for geometric modelling, chapter surface parameterization: a tutorial and survey, pp 157–186. Springer
6. Greson J, Sheffer A, Zhang E (2011) All-hex mesh generation via volumetric polycube deformation. Comput Graph Forum 30(5):1407–1416
7. Grinspun E, Schröder P, Desbrun M (2005) Discrete differential geometry: an applied introduction. In: ACM SIGGRAPH'05 course notes
8. Gu X, Yau S-T (2003) Global conformal parameterization. In: Symposium on geometry processing, pp 127–137

9. Guo Y, Pan Y (2005) Harmonic maps based constrained texture mapping method. CAD & CG (Chinese) 17(7):1457–1462
10. Guo Y, Wang J, Sun H, Peng Q (2005) A novel constrained texture mapping method based on harmonic map. Comput Graph 29(6):972–979
11. Han S, Xia J, He Y (2010) Hexahedral shell mesh construction via volumetric polycube map. In: Proc of the 14th ACM symposium on solid and physical modeling, pp 127–136
12. Han S, Xia J, He Y (2011) Constructing hexahedral shell meshes via volumetric polycube maps. Comput Aided Des 43(10):1222–1233
13. He Y, Wang H, Fu C-W, Qin H (2009) A divide-and-conquer approach for automatic polycube map construction. Comput Graph 33(3):369–380
14. Lai Y-K, Jin M, Xie X, He Y, Palacios L, Zhang E, Hu S-M, Gu X (2010) Metric-driven rosy field design and remeshing. IEEE Trans Vis Comput Graph 16(1):95–108
15. Nieser M, Reitebuch U, Polthier K (2011) Cubecover—parameterization of 3d volumes. Comput Graph Forum 30(5):1397–1406
16. Radó, T (1926) Aufgabe 41. Jahresber Deutsch Math-Verein 35(49):49
17. Sarkar R, Zeng W, Gao J, Gu XD (2010) Harmonic quorum systems: Data management in 2d/3d wireless sensor networks with holes. In: Proceedings of the 9th ACM/IEEE International conference on information processing in sensor networks, pp 232–243
18. Sheffer A, Praun E, Rose K (2006) Mesh parameterization methods and their applications. Foundations and Trends in Computer Graphics and Vision 2(2):105–171
19. Si H (2009) Tetgen: a quality tetrahedral mesh generator and three-dimensional delaunay triangulator. Software available at http://tetgen.org
20. Sorkine O, Alexa M (2007) As-rigid-as-possible surface modeling. In: Proceedings of the fifth eurographics symposium on geometry processing, pp 109–116
21. Tarini M, Hormann K, Cignoni P, Montani C (2004) Polycube-maps. ACM Trans Graph 23(3):853–860
22. Tigges M, Wyvil B (1999) A field interpolated texture mapping algorithm for skeletal implicit surfaces. In: Computer graphics international 1999, pp 25–32
23. Tobias M, Cohen E, Kirby M. (2008) Volumetric parameterization and trivariate b-spline fitting using harmonic functions. In: Proc of the 2008 ACM symposium on solid and physical modeling, pp 269–280
24. Tong Y, Alliez P, Cohen-Steiner D, Desbrun M (2006) Designing quadrangulations with discrete harmonic forms. In: Symposium on geometry processing, pp 201–210
25. Turk G, O'Brien JF (1999) Shape transformation using variational implicit functions. In: Proc of ACM SIGGRAPH 1999, pp 335–342
26. Wang Y, Gu X, Thompson PM, Yau S-T (2004) 3d harmonic mapping and tetrahedral meshing of brain imaging data. In: Proc of medical imagng computing and computer assisted intervention, pp 26–30
27. Wang H, He Y, Li X, Gu X, Qin H (2007) Polycube splines. In: Proceedings of the 2007 ACM symposium on solid and physical modeling, pp 241–251
28. Wang H, He Y, Li X, Gu X, Qin H (2007) Polycube splines. Comput Aided Des 40(6):721–733
29. Xia J, He Y, Han S, Fu C-W, Luo F, Gu X (2010) Parameterization of star shaped volumes using green's functions. In: Geometric modeling and processing 2010, pp 219–235
30. Xia J, He Y, Yin X, Han S, Gu X (2010) Direct-product volumetric parameterization of handle-bodies via harmonic fields. In: Proc of shape modeling international conference, pp 3–12
31. Xin L, Guo X, He Y, Gu X, Qin H (2007) Harmonic volumetric mapping for solid modeling applications. In: Proceedings of the 2007 ACM Symposium on solid and physical modeling, pp 109–120
32. Xin L, Guo X, Wang H, He Y, Gu X, Qin H (2009) Meshless harmonic volumetric mapping using fundamental solution methods. IEEE Trans Autom Sci Eng 6(3):409–422
33. Xu D, Zhang H, Wang Q, Bao H (2005) Poisson shape interpolation. In: Proc of the 2005 ACM Symposium on solid and physical modeling, pp 267–274
34. Zhang C, Luo J, Xiang L, Li F, Lin J, He Y (2012) Harmonic quorum systems: Data management in 2d/3d wireless sensor networks with holes. In: Proceedings of 2012 9th Annual IEEE Communications society conference on sensor, mesh and ad hoc communications and networks (SECON), pp 1–9
35. Zeng W, Marino J, Kaufman AE, Gu X (2011) Volumetric colon wall unfolding using harmonic differentials. Comput Graph 35(3):726–732

**Juncong Lin**  is now an associate professor at Xiamen University. He received the Ph.D. degree in Computer Science from Zhejiang University. His research interests include geometry processing and sketch based modeling.
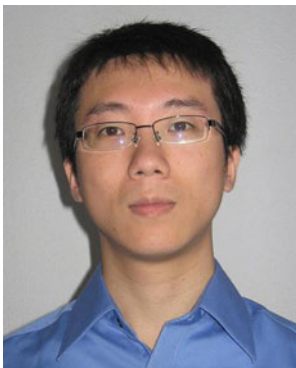


**Jiazhi Xia**  received the BS and MS degrees in Computer Science from Zhejiang University, China, and the PhD degree in Computer Science from Nanyang Technological University. He is currently a lecturer at the School of Information Science and Engineering, Central South University, China. His research interests include computer graphics, multimedia, and human-computer interaction.

**Xing Gao** is now an assistant professor at Xiamen University, P.R.China. He received the Ph.D. degree in Computer Science from Harbin Institute of Technology. His research interests include sketch based modeling.



**Minghong Liao** is a professor of Software School of Xiamen University. He received his Ph.D. degree in Computer Science in 1993 from Harbin Institute of Technology of China. His research interests include Intelligent Network, Pervasive Computing and Computer Graphics.

**Ying He** received the BS and MS degrees in Electrical Engineering from Tsinghua University, China, and the PhD degree in Computer Science from the State University of New York (SUNY), Stony Brook. He is an associate professor at NTU, Singapore. His research interests fall in the broad area of visual computing.



**Xianfeng Gu** received the PhD degree in computer science from Harvard University in 2003. He is an assistant professor of computer science and the director of the 3D Scanning Laboratory in the Department of Computer Science at Stony Brook University, New York. His research interests include computer vision, graphics, geometric modeling, and medical imaging. His major works include global conformal surface parameterization in graphics, tracking and analysis of facial expression in vision, manifold splines in modeling, brain mapping and virtual colonoscopy in medical imaging, and computational conformal geometry. He won the US National Science Foundation CAREER Award in 2004. He is a member of the IEEE.